Original Article

The Effect of Selenium Nanoparticles versus Royal Jelly against Cisplatin-Induced Testicular Toxicity in Adult Male Albino Rats: A Light and Transmission Electron Microscopic Study

Christina S. Eisa, Sally S. Mohammed, Hoida I. Abd El-Aziz, Lamia M. Farghaly, Somaya Hosny
Department of Histology and Cell Biology, Faculty of Medicine, Suez Canal University, Ismailia, Egypt

Abstract

Background and Aim: Cisplatin (Cis) is a highly effective chemotherapeutic agent. However, it produces severe testicular toxicity. It was reported that some antioxidants could overcome this toxicity. Selenium nanoparticles and royal jelly (RJ) were among these reported antioxidants. Therefore, this study was designed to compare these two antioxidants in protecting the testes against Cis-induced toxicity. **Materials and Methods:** This study was conducted on sixty healthy adult male albino rats (weight: 200–220 g) randomized into six groups, ten animals each. Group I (control), Group II (animals received intragastric Nano Selenium), Group III (animals received intragastric RJ), Group IV (animals received an IP injection of Cis 7 mg/kg), Group V (animals received intragastric Nano Selenium, and Cis injection), and Group VI (animals received intragastric RJ and Cis injection). After 10 days, the animals were sacrificed by cervical decapitation. The testes were weighted, and specimens from the left testis were processed for histological and immunohistochemical techniques, whereas specimens from the right testes were prepared for transmission electron microscopic examination. **Results:** Cis-treated animals had significantly reduced weight of their testes. Light microscopic examination revealed severe histopathological changes in the germinal epithelium and Leydig cells, confirmed with electron microscopic examination. There was a significant increase in the color area percentage of Caspase-3 immunostaining of the germinal epithelium and Leydig cells, compared to that of the control group. Group II and III were similar to control group. Both Groups V and VI revealed significant preservation compared to the Cis group. **Conclusion:** Selenium nanoparticles and RJ partially improved testis from Cis-induced toxicity, However, there was no significant difference between both groups.

Keywords: Caspase 3, cisplatin testicular damage, electron microscope, royal jelly, selenium nanoparticles

Introduction

Cisplatin (Cis) is a highly effective and commonly used DNA alkylating chemotherapeutic agent for the treatment of diverse types of solid tumors. However, it was found to produce severe testicular toxicity through disruptions of the redox balance of testicular tissues.[1] This damage was in the form of germ cell apoptosis, Leydig cell dysfunction, and testicular steroidogenic disorder causing infertility. In addition, spermatogenesis was affected, as Cis inhibited nucleic acid synthesis in germ cells.[2]

Interestingly, growing evidences revealed that combination therapy of Cis with antioxidants can be beneficial to overcome this special reproductive toxicity.[1] Some antioxidants were shown to protect against Cis toxicity such as curcumin,[3] ginger,[4] royal jelly (RJ),[5] and selenium.[6]

Selenium (Se) is a micronutrient that is known to have antioxidant capabilities. However, it has a narrow range between therapeutic and toxic doses. Therefore, selenium nanoparticles (Nano Se) have been introduced as alternatives for selenocompounds due to their excellent lower toxicity and higher antioxidant effects.[7]

Address for correspondence: Dr. Sally S. Mohammed, Faculty of Medicine, Suez Canal University, Circular Road, Ismailia, Egypt.
E-mail: sallysalem@med.suez.edu.eg

Received: 12-05-2021 **Revised:** 25-07-2021
Accepted: 19-08-2021 **Published:** 23-05-2022

Access this article online

Quick Response Code:

Website: http://www.jmau.org/

DOI: 10.4103/jmau.jmau_44_21

How to cite this article: Eisa CS, Mohammed SS, Abd El-Aziz HI, Farghaly LM, Hosny S. The effect of selenium nanoparticles versus royal jelly against cisplatin-induced testicular toxicity in adult male albino rats: A light and transmission electron microscopic study. J Microsc Ultrastruct 2022;10:180-96.

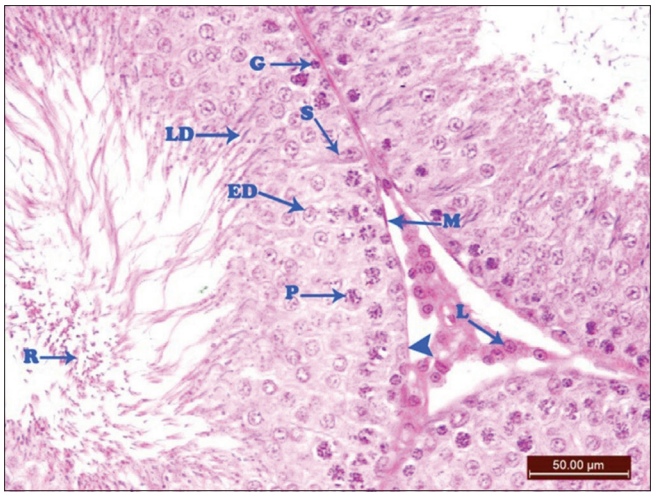

Figure 1: Photomicrograph of seminiferous tubules from Group I. The tubules are closely packed, have sperms® and are lined with all germinal epithelium resting on regular well-defined basement membrane (arrow head); spermatogonia (G) are small with rounded opaque or open face nuclei, Sertoli cells (S) are tall cells with open face oval nuclei, 1ry spermatocytes (P) are large rounded cells, early spermatids (ED) are small rounded cells with vesicular round nuclei and late spermatids (LD) with elongated dark nuclei. The tubules are surrounded by flat myoid cells (M) and are separated by narrow spaces containing clusters of polyhedral Leydig cells (L) with rounded vesicular nuclei and eosinophilic cytoplasm (H and E, ×400)

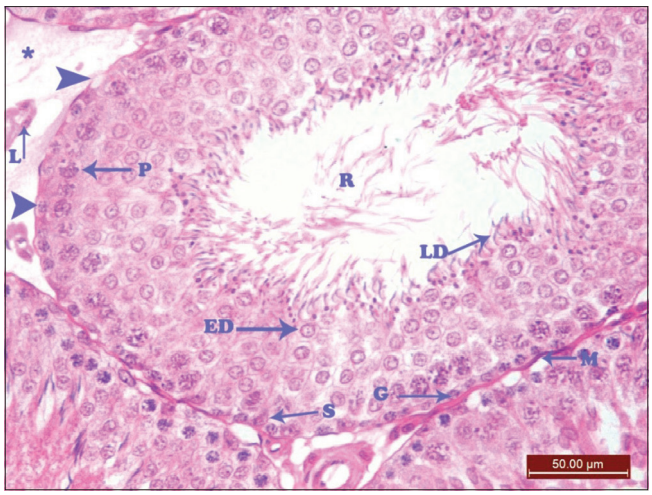

Figure 3: Photomicrograph of seminiferous tubules from Group V showing evidence of improvement. The tubule is lined with all layers of the germinal epithelium; spermatogonia (G), Sertoli cells (S), 1ry spermatocytes (P), early spermatids (ED), and late spermatids (LD). It contains sperms® and is surrounded by a basement membrane and flattened myoid cells (M). The basement membrane still shows some corrugations (arrow head). The interstitial space (*) shows shrunken Leydig cells (L) (H and E, ×400)

Previous studies found that Nano Se could improve sperm count, motility, and vitality in mice. This improvement in spermatic parameters was attributed to the antioxidant effects of Nano Se.[8] Another study showed that supplementation with elemental Nano Se resulted in protection against chemotherapy-induced reproductive toxicity.[9]

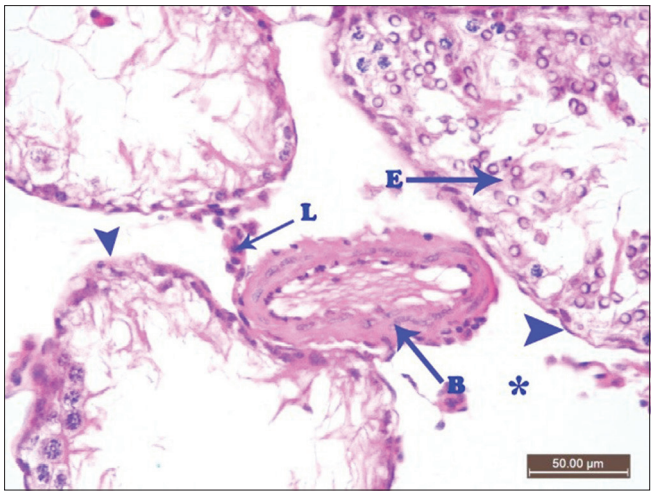

Figure 2: Photomicrograph of seminiferous tubules from Group IV showing disorganization, detachment, or loss of the germinal epithelium (E). The basement membrane is corrugated (arrow head). The interstitial spaces are wide (*) with a thickened blood vessel (B) and shrunken Leydig cells (L) that show pyknotic nuclei (H and E, ×400)

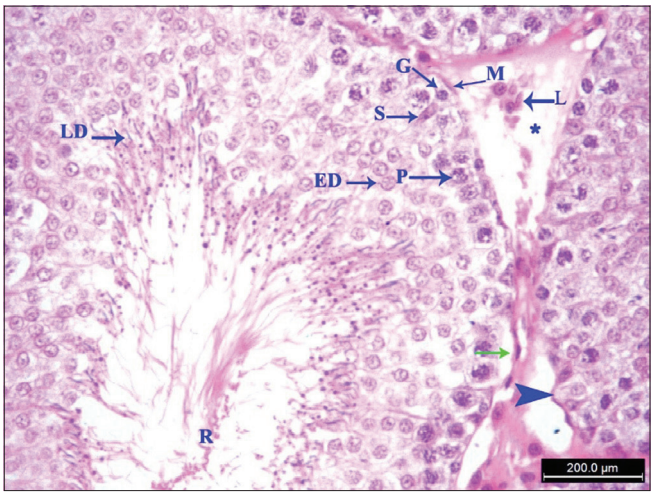

Figure 4: Photomicrograph of seminiferous tubules from Group VI showing evidence of improvement. The tubule is lined with all cells of germinal epithelium; spermatogonia (G), Sertoli cells (S), 1ry spermatocytes (P), early spermatids (ED), and late spermatids (LD). It contains sperms® and is surrounded by a basement membrane showing flattened myoid cells (M). Areas of separation (green arrows) of the cells from the basement membrane and few corrugations (arrow head) of the basement membrane are still noticed. The interstitial space showing Leydig cells (L) with rounded vesicular nuclei (H and E, ×400)

RJ is the principal food of the queen honeybees, which is secreted by the hypo pharyngeal and mandibular glands of the young nurse worker bees. It possesses multiple pharmacological properties including antioxidant, antitumor, antibiotic, anti-inflammatory, hypotensive, and immunomodulatory activities. In addition, some studies showed that RJ has positive effects on the reproductive system and fertility in humans and animals.[10]

Limited histological studies were conducted to investigate the protective role of RJ and Nano Se against Cis-induced

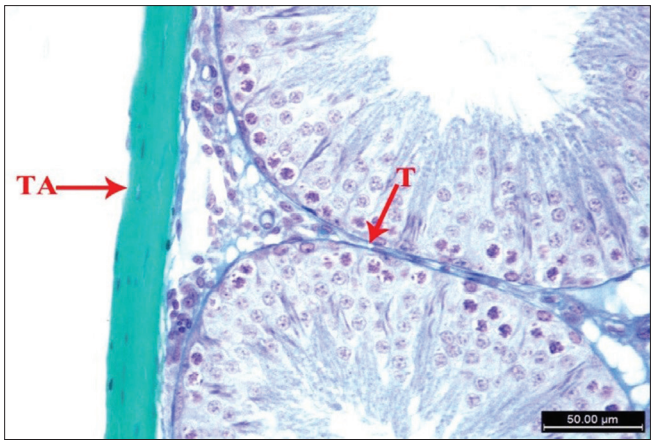

Figure 5: Photomicrograph from Group I testis showing the normal greenish color of the connective tissue of the tunica albuginea (TA) and the walls of the seminiferous tubules (T) (Masson's trichrome, ×400)

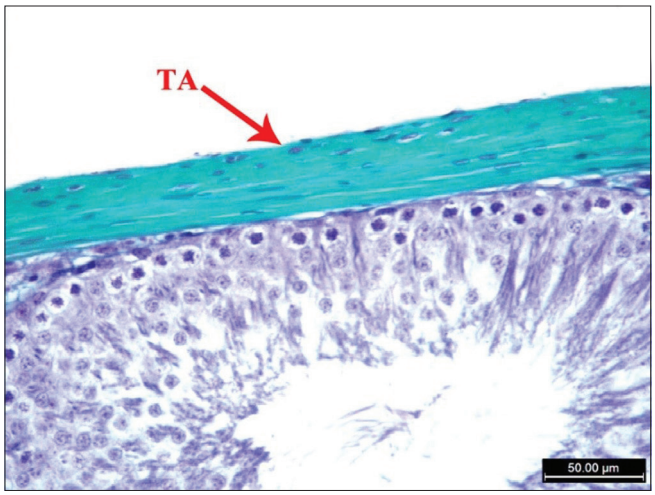

Figure 7: Photomicrograph from Group V testis showing the greenish color of the connective tissue of the tunica albuginea (TA), nearly similar to that of the control group (Masson's trichrome, ×400)

testicular toxicity. In addition, there are no available studies to compare the protective roles of RJ or Nano Se against Cis -induced testicular toxicity. Hence, the present work was designed to study and compare the possible protective effects of RJ and Nano Se against Cis-induced testicular toxicity using light and electron microscopies.

Materials and Methods

Drugs

Cis was purchased from the pharmacy in the form of Cis e Mylan vials 50 mL (1 mg/1 mL), Penta Pharma Industries, Lebanon.

Selenium nanoparticles were purchased from Nano-Tech, Cairo, Egypt. They were prepared in suspension form at a concentration of 0.4 mg/mL.

RJ was purchased from YS Organic Bee Farms, Sheridan, IL, USA, in a semisolid form and was prepared by dispersion in distilled water.

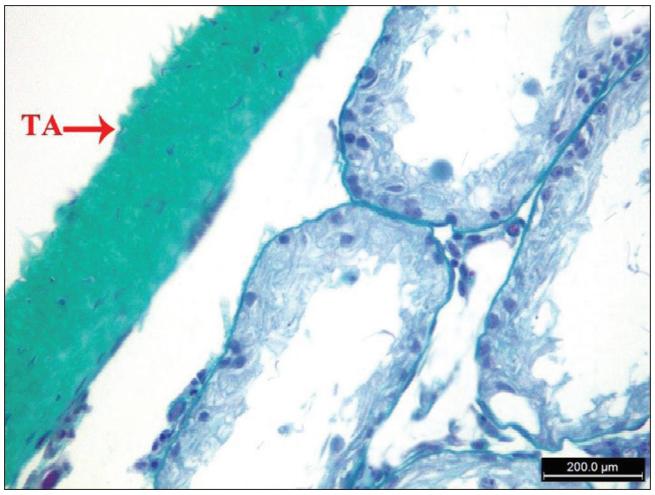

Figure 6: Photomicrograph from Group IV testis showing greenish thickened tunica albuginea with irregular fibers (TA) (Masson's trichrome, ×400)

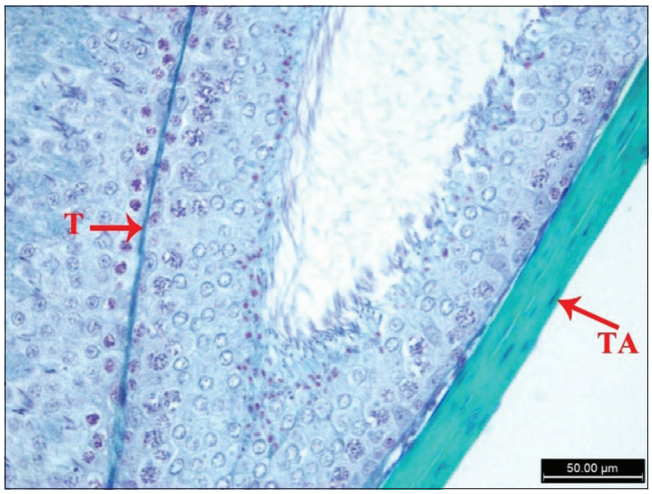

Figure 8: Photomicrograph from Group VI testis showing the greenish color of the connective tissue of the tunica albuginea (TA) and the wall of a seminiferous tubule (T), nearly similar to the control group (Masson's trichrome, ×400)

Animals and study design

This study was conducted on sixty healthy adult male albino rats of same age and weight (200–220 g), purchased from the animal house of the Faculty of Veterinary Medicine, Suez Canal University. They were acclimatized for 7 days before the experiment with free access to food and water, and housed in clean cages at ordinary room temperature.

After acceptance from the research and ethics committee of the Faculty of Medicine, Suez Canal University, the animals were randomized into six groups, ten animals each. Group I (control group) received a single IP injection of distilled water at a dose of 7 mL/kg. Group II (Nano Se group) received intragastric Nano Se dispersed in distilled water, orally via gavage at a dose of 2 mg/kg/day for 10 days.[9] Group III (RJ group) received intragastric RJ dispersed in distilled water, orally via gavage at a dose of 100 mg/kg/day for 10 days.[5] Group IV (Cis group)

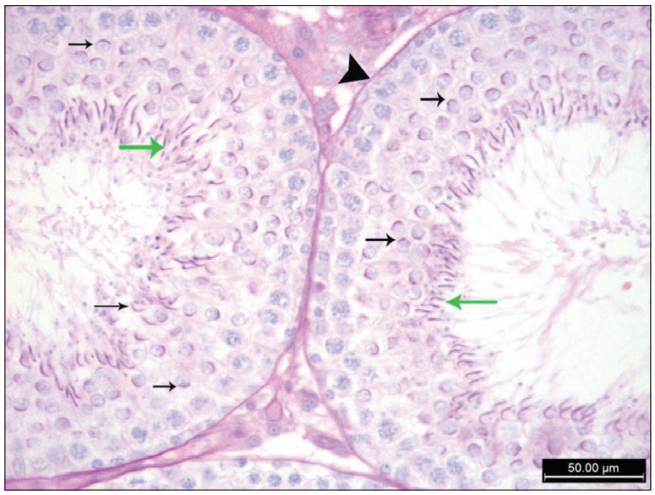

Figure 9: Photomicrograph from Group I testis showing PAS + ve regular basement membrane (arrow head), caps of early spermatids (black arrows), and heads of late spermatids (green arrows) (PAS, ×400)

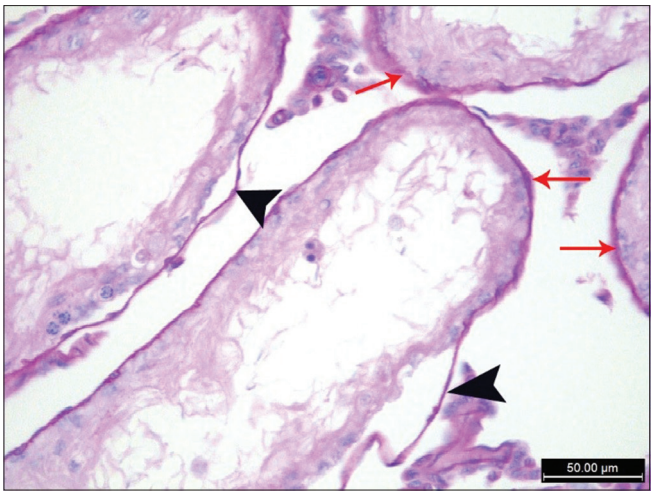

Figure 10: Photomicrograph from Group IV testis showing PAS + ve basement membrane with areas of corrugation and separation from the germinal epithelium (arrowhead) and multiple areas of thickening (red arrows) (PAS, ×400)

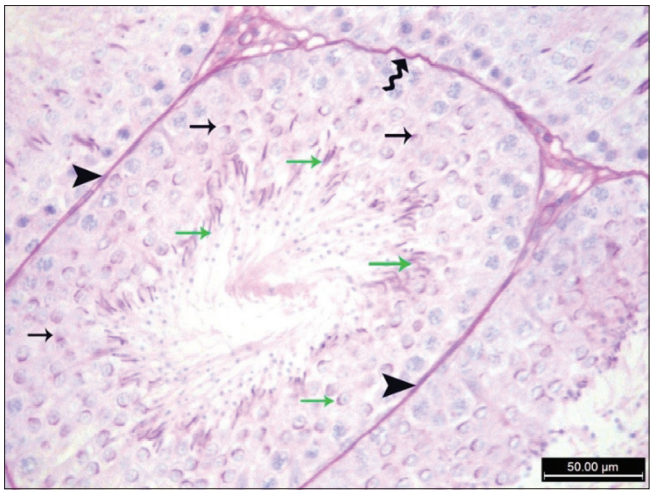

Figure 11: Photomicrograph from Group V testis showing almost regular PAS + ve basement membrane (arrowhead) with few areas of corrugations (wavy arrow). PAS + ve caps of early spermatids (black arrows) and heads of late spermatids (green arrows) are also shown (PAS, ×400)

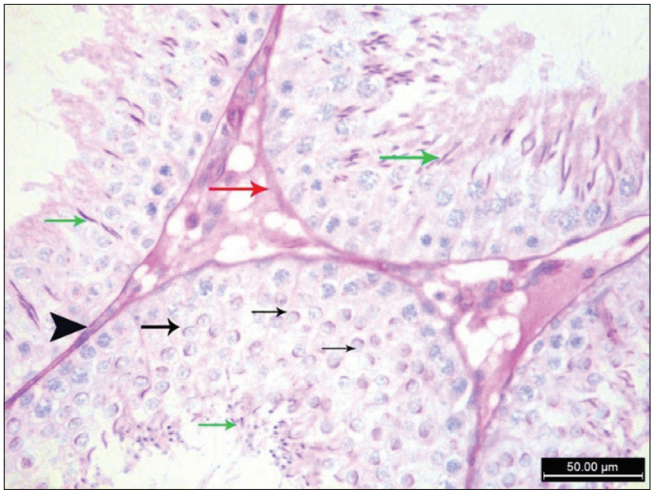

Figure 12: Photomicrograph from Group VI testis showing almost regular PAS + ve basement membrane (arrowhead) with few areas of thickening (red arrow). PAS + ve caps of rounded spermatid (black arrows) and heads of elongated spermatids (green arrows) are also shown (PAS, ×400)

received a single IP injection of Cis at a dose of 7 mg/kg.[9] Group V (Cis + Nano Se group) received a single IP injection of Cis at a dose of 7 mg/kg followed by intragastric administration of Nano Selenium dispersed in distilled water, orally via gavage at a dose of 2 mg/kg/day for 10 days.[9] Group VI (Cis + RJ group) received a single IP injection of Cis at a dose of 7 mg/kg followed by intragastric administration of RJ dispersed in distilled water, orally via gavage at a dose of 100 mg/kg/day for 10 days.[5]

Specimen collection and the used histological techniques

At the end of the experiment, all animals were anesthetized with ether and then sacrificed by cervical decapitation. The testes were weighed, and specimens from the left testes were obtained and processed for light microscopic (LM) examination using hematoxylin and eosin (H and E), Masson's trichrome, periodic acid–Schiff (PAS), and caspase-3 immunostaining, whereas specimens from the right testes were processed for transmission electron microscopic (TEM) examination.

For caspase 3 immunostain

Assessment of apoptosis was done by the detection of caspase-3 protein in the cytoplasm of the germinal epithelium cells and Leydig cells. The primary antibody was rabbit poly clonal antibody to caspase-3 (cat. RB-1197-P0), purchased from Thermo Scientific™ Lab Vision™, USA, by its supplier in Egypt, Midco Trade Company. The detection kit (Power-Stain™ 1.0 Poly HRP DAB Kit for Mouse + Rabbit) was purchased from Genemed Biotechnologies Inc.

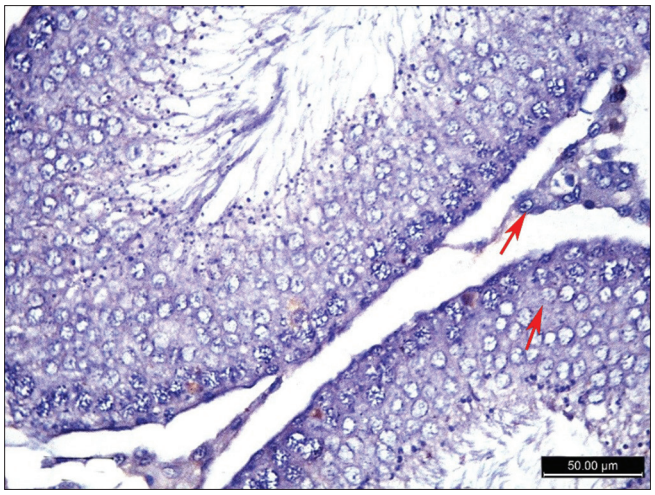

Figure 13: Photomicrograph from Group I testis showing almost negative cytoplasmic immunoreactivity of the germinal epithelium cells and Leydig cells (red arrows) (Caspase-3 immunostaining, ×400)

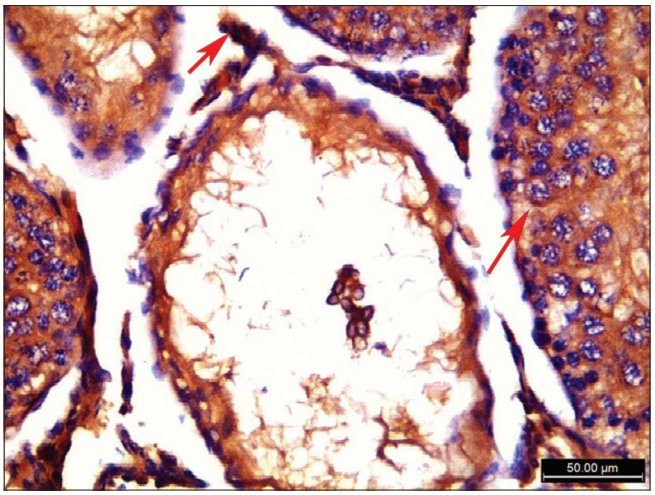

Figure 14: Photomicrograph from Group IV testis showing strong brown cytoplasmic immunoreactivity of the germinal epithelium cells and Leydig cells (red arrows) (Caspase-3 immunostaining, ×400)

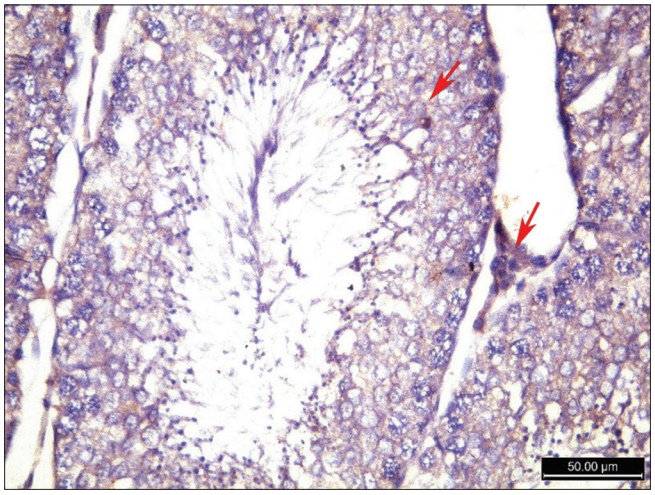

Figure 15: Photomicrograph from Group V testis showing weak brownish cytoplasmic immunoreactivity of the germinal epithelium cells and Leydig cells (red arrows), compared to the Cis group (Caspase-3 immunostaining, ×400)

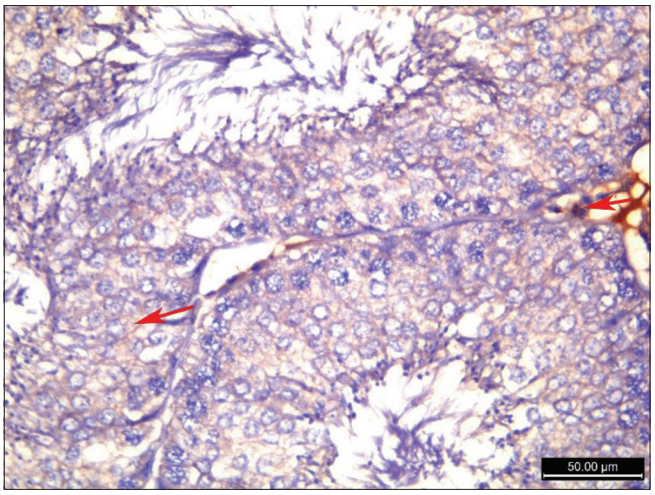

Figure 16: Photomicrograph from Group VI testis showing weak brownish cytoplasmic immunoreactivity of the germinal epithelium cells and Leydig cells (red arrows), compared to the Cis group (Caspase-3 immunostaining, ×400)

For negative control, the same protocol was followed with omission of the primary antibody step.

For positive control, tonsils tissue was stained following the same protocol.

Histopathological and Morphometric study

Quantitative assessment

Five fields per section and three sections per animal were analyzed by computer-assisted image analysis, the pro-plus software, at the Histology Department of Faculty of Medicine in Suez Canal University. A magnification of ×100 was used or the 1st and 2nd parameters and a magnification of ×400 for the 3rd and 4th parameters:[9]

- Diameter of the seminiferous tubules in H and E-stained sections
- Germinal epithelium thickness in H and E-stained sections
- Color area percentage of caspase-3 immunoreactivity (brownish color) among all groups
- Optical density of caspase-3 immunoreactivity (brownish color) among Cis-receiving groups.

Qualitative assessment

General architecture histopathological changes of the testes

Five fields per H and E-stained section and three sections per animal were examined by light microscope to assess the following histopathological changes, and the frequency distribution of each change was calculated:[5]

- Loss of architecture
- Thickening of tunica albuginea
- Congestion of blood vessels
- Widening of interstitial spaces

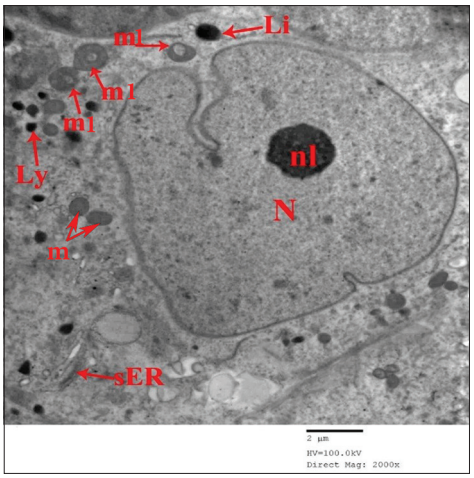

Figure 17: Electron photomicrograph of a Sertoli cell from Group I showing a large indented euchromatic nucleus (N) with a prominent nucleolus (nl). The cytoplasm shows rounded mitochondria (m) with some of them showing doughnut-shaped appearance (m1). Some lysosomes (Ly), lipid droplets (Li), and smooth endoplasmic reticulum (sER) are also shown in the cytoplasm (TEM, ×2000)

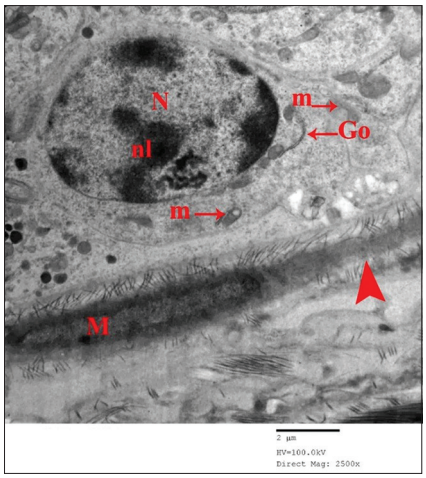

Figure 18: Electron photomicrograph of a spermatogonium from Group I resting on a regular basement membrane (arrow head) with flat myoid cell (M). It shows a regular oval nucleus (N) with condensed chromatin arranged peripherally and around the nucleolus (nl). The cytoplasm shows mitochondria (m) and Golgi apparatus (Go) (TEM, ×2500)

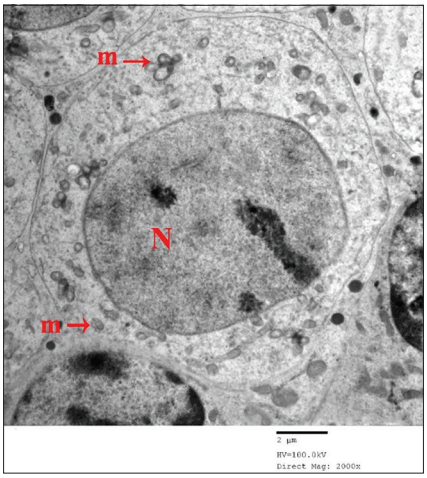

Figure 19: Electron photomicrograph of a primary spermatocyte from Group I. It is large, rounded with a central large regular rounded nucleus (N) in the prophase of the first meiotic division. The cytoplasm shows numerous mitochondria (m) (TEM, ×2000)

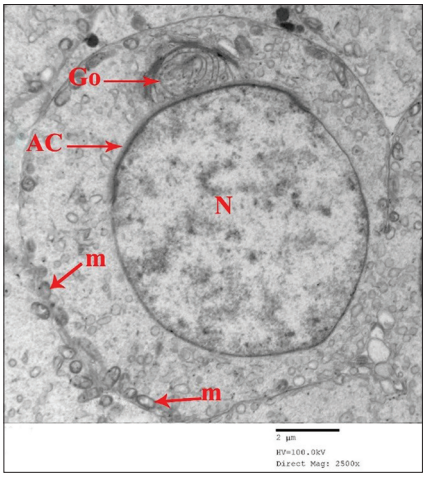

Figure 20: Electron photomicrograph of an early spermatid from Group I. It appears as a rounded cell with a rounded nucleus (N) covered anteriorly with acrosomal cap (AC). The nucleus occupies most of the cytoplasm that shows numerous mitochondria (m) arranged peripherally and a Golgi apparatus (Go) near the nucleus (TEM, ×2500)

- Leydig cell affection (shrinkage and/or nuclear changes).

Seminiferous tubule histopathological changes

Thirty random seminiferous tubules per animal were examined at high-power field (×400), and the following histopathological changes were assessed, and then the percentage of each change was calculated:[11]

- Corrugation of basement membrane
- Separation of germinal epithelium from the basement membrane and from each other
- Partial, extensive, or loss of germinal epithelium
- Sloughing of germinal epithelium into seminiferous tubule lumen
- Cytoplasmic vacuolations
- Nuclear changes; pyknosis, karyolysis, and chromatin margination.

Statistical analysis

Quantitative variables were presented as mean and standard deviation and qualitative variables were presented as frequency and percentage, and the difference among the studied groups was presented by tables and graphs.

The difference among the six groups considering the frequency distribution of histopathological changes in the testicular tissue was tested for significance by using Chi-square test and then pairwise comparisons were performed using Fisher's exact test. In addition, the difference among the four groups considering the testes weight and quantitative assessment of

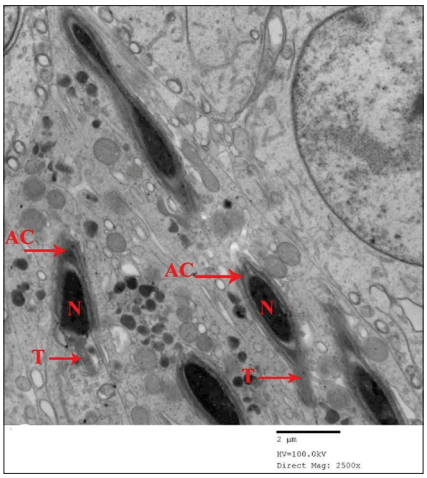

Figure 21: Electron photomicrograph of late spermatids from Group I. Each spermatid shows almost a pyriform electron-dense nucleus (N) covered anteriorly with an acrosomal cap (AC). The caudal parts of spermatids show the elongating tails (T) (TEM, ×2500)

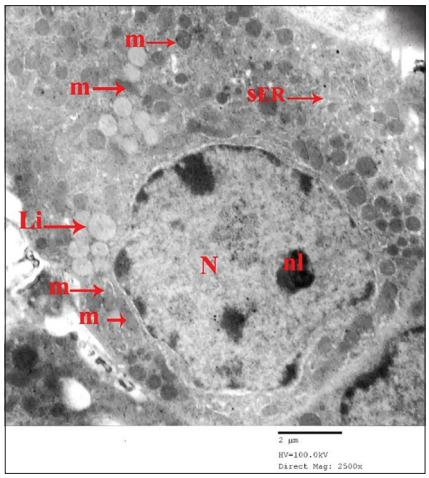

Figure 22: Electron photomicrograph of a Leydig cell from Group I. It shows an almost rounded regular nucleus (N), with predominant euchromatin and a nucleolus (nl). The cytoplasm shows numerous mitochondria (m), lipid droplets (Li), and well-developed smooth endoplasmic reticulum (sER) (TEM, ×2500)

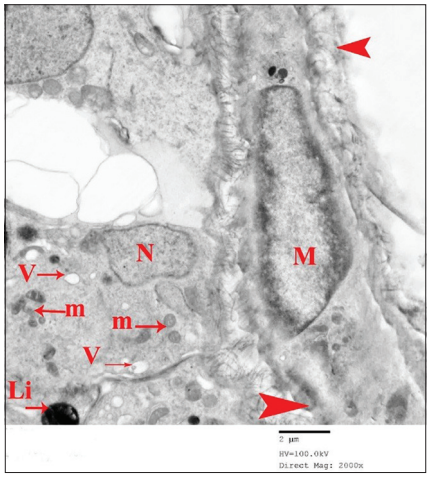

Figure 23: Electron photomicrograph of a Sertoli cell from Group IV showing a shrunken eccentric nucleus (N). The cytoplasm shows multiple vacuoles (V) and a large electron-dense lipid droplet (Li). Some mitochondria (m) are also shown in the cytoplasm. The cell rests on a thickened irregular basement membrane (arrowhead), compared to that of the control group, with a thickened myoid cell (M) which shows margination of nuclear chromatin (TEM, ×2000)

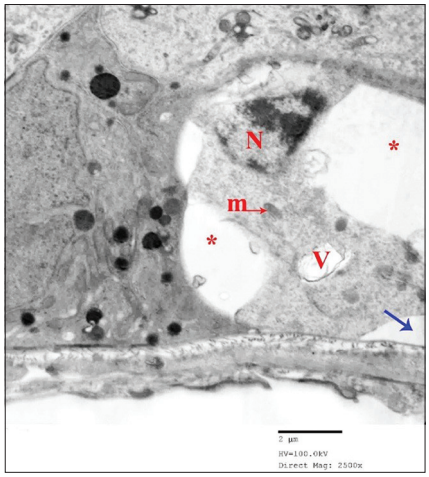

Figure 24: Electron photomicrograph of a spermatogonium from Group IV. The cell shows an irregular dark shrunken nucleus (N) and vacuolated cytoplasm (V). Areas of separation (asterisk) from neighboring cells and detachment (blue arrow) from the basement membrane are shown. Some mitochondria (m) are also shown in the cytoplasm (TEM, ×2500)

the seminiferous tubules was tested for significance by using Kruskal–Wallis test and then *post hoc* pairwise comparisons were performed using adjusted Bonferroni approach. Statistical significance was considered at $P < 0.05$.

Results

Weight of testes

The weight of the testes markedly decreased in the Cis group (Group IV) compared to that of the control group (Group I). Cis + Nano Se (Group V) and Cis + RJ (Group VI) groups showed minimal weight decrease compared to that of the control group. However, there was no statistically significant difference between Groups V and VI [Graph 1].

Light microscopic results

Hematoxylin and eosin results

The control group showed normal architecture of the testes in 100% of animals. Each testis was formed by multiple regular and closely packed seminiferous tubules and separated by narrow interstitial spaces containing normal Leydig cells. Each seminiferous tubule was full of sperms and lined with stratified germinal epithelium resting on a regular, well-defined basement membrane [Figure 1 and Table 1]. The mean thickness of the germinal epithelium was 99.2 μm and the mean diameter of the seminiferous tubules was 281.3 μm [Table 2].

Groups II and III showed testicular structure similar to that of the control group.

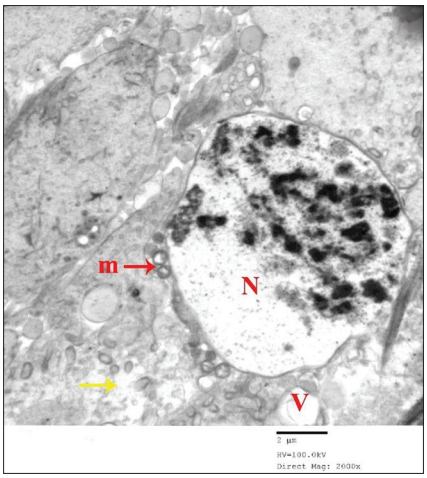

Figure 25: Electron photomicrograph of a primary spermatocyte from Group IV. It shows an irregular nucleus (N) with dark fragmented chromatin. The cytoplasm is disintegrated (yellow arrow) and vacuolated (V). Some mitochondria (m) are also shown in the cytoplasm (TEM, ×2000)

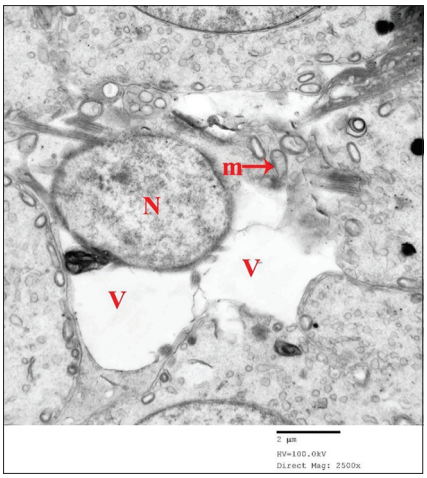

Figure 26: Electron photomicrograph of an early spermatid from Group IV. It shows a shrunken rounded-to-oval nucleus (N) that lacks an acrosomal cap. The cytoplasm is massively vacuolated (V) and the remnants of cytoplasm show few mitochondria (m) (TEM, ×2500)

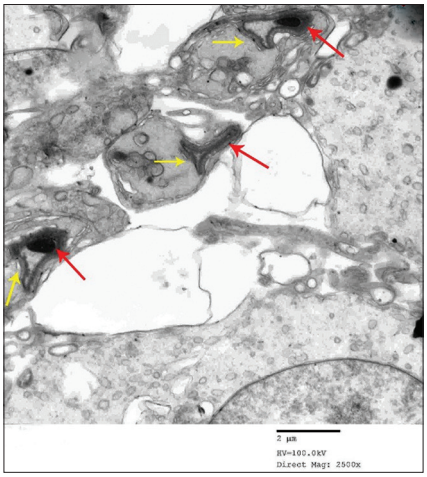

Figure 27: Electron photomicrograph of late spermatids from Group IV. The spermatids are deformed with decreased condensation of their nuclei (red arrows). The caudal parts of the spermatids lack the elongating tails (yellow arrows) (TEM, ×2500)

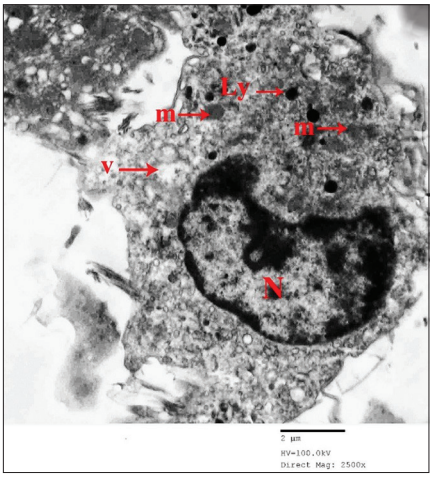

Figure 28: Electron photomicrograph of a Leydig cell from Group IV. It has an irregular dark shrunken nucleus (N) and vacuolated cytoplasm (V). There are multiple lysosomes (Ly) and few mitochondria (m) in the cytoplasm. No lipid droplets are shown (TEM, ×2500)

Group IV (Cis group) showed loss of testes architecture in 50% of the animals. Most of the counted seminiferous tubules appeared shrunken and irregular. Widening of the interstitial spaces among the seminiferous tubules and thickened congested blood vessels were noticed in 80% of the animals. The Leydig cells were shrunken with pyknotic nuclei.

Most of the seminiferous tubules showed corrugated basement membrane and partial loss of the germinal epithelium. The epithelium was disorganized and detached from the basement membrane. The frequency distribution of all histopathological changes in this group is shown in Table 1. There was a significant decrease in the mean thickness of the germinal epithelium and the mean diameter of the seminiferous tubules, compared to the control group [Figure 2 and Table 2].

Table 1: Frequency distribution (%) of the histopathological changes of testicular tissues among the six experimental groups

Group	I	II	III	IV	V	VI	*P*
Thickening of tunica albuginea	0	0	0	80#	10@	20@	<0.001*
Blood vessel congestion	0	0	0	80#	20@	20@	<0.001*
Wide spaces among tubules	0	0	0	80#	10@	20@	<0.001*
Leydig cells necrosis	0	0	0	90#	20@	30@	<0.001*
Loss of architecture	0	0	0	50#	0@	10@	<0.001*

*Statistically significant at $P<0.05$, #Statistically significant compared to Group I, @Statistically significant compared to Group IV, Chi-square test

Group V (Cis + Nano Selenium) showed evidence of improvement. All animals showed preserved architecture of the testis. The tunica albuginea appeared thin in most of the

Table 2: Seminiferous tubules' histopathological changes among the six experimental groups in H and E-stained sections presented, as mean±standard deviation

Group	I	II	III	IV	V	VI	*P*
Assessment of qualitative parameters of the seminiferous tubules (%)							
Basement membrane corrugation	1.3±2.3	1.3±2.3[@]	2±2.8[@]	81.3±15.7[#]	23.6±5.8[#,@]	27.7±6.7[#,@]	<0.001*
Separation of germinal epithelium from basement membrane	2±2.8	2±3.6[@]	2±3.6[@]	79.7±18.1[#]	21.7±5.9[#,@]	27.7±9.4[#,@]	<0.001*
Separation of germinal epithelium cells from each other	1.7±2.6	2±2.8[@]	2±3.2[@]	78.3±17.7[#]	20.3±5.3[#,@]	26.7±5.4[#,@]	<0.001*
Partial loss of germinal epithelium	2±2.8	2±3.6[@]	2±3.6[@]	60.1±29.6[#]	20±8.7[#,@]	26±7.8[#,@]	<0.001*
Extensive loss of germinal epithelium	0±0	0±0[@]	0±0[@]	32.7±32.1[#]	3.5±6.4[#,@]	3.7±5.5[#,@]	<0.001*
Sloughing of germinal epithelium into the lumen	0.3±1.1	1±2.3[@]	1.3±3.2[@]	54.9±28.1[#]	10.3±7.3[#,@]	14.7±5[#,@]	<0.001*
Cytoplasmic vacuolation	2.3±3.2	2±3.6[@]	2±3.6[@]	89.7±14.3[#]	30±7.4[#,@]	30.3±3.3[#,@]	<0.001*
Nuclear changes	2.3±3.2	2±3.6[@]	2±3.6[@]	88±13.9[#]	27.3±4.7[#,@]	29±8.5[#,@]	<0.001*
Shrinkage of seminiferous tubules	0±0	0.7±1.4[@]	0.7±1.4[@]	84±39.9[#]	14.7±3.9[#,@]	16±8.1[#,@]	<0.001*
Assessment of quantitative parameters of the seminiferous tubules							
Diameter of seminiferous tubules	281.3±16.6	274.2±6.9[@]	276.3±11.1[@]	141.3±13.5[#]	242.4±11.1[#,@]	232.5±13.5[#,@]	<0.001*
Thickness of germinal epithelium	99.2±8.3	97.5±5.9[@]	95.5±6.7[@]	30.3±7.4[#]	59±6.4[#,@]	57.6±9.2[#,@]	<0.001*

*Statistically significant at $P<0.05$, [#]Statistically significant when compared with Group I, [@]Statistically significant when compared with Group IV, Kruskal-Wallis test. *Post hoc* pairwise comparisons used adjusted Bonferroni approach

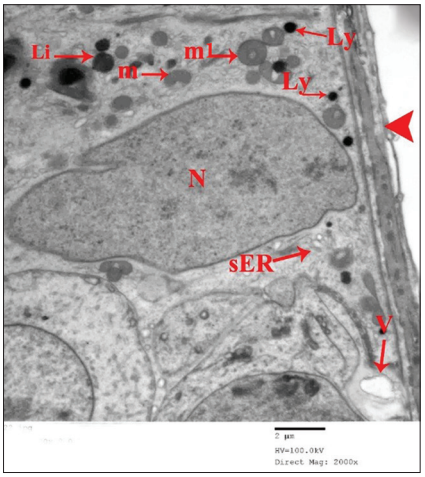

Figure 29: Electron photomicrograph of a Sertoli cell from Group V showing evidence of improvement. The cell rests on a regular basement membrane (arrowhead). It shows a large indented euchromatic nucleus (N). The cytoplasm shows mitochondria (m) that sometimes show the doughnut-shaped appearance (m1). Some lysosomes (Ly) and smooth endoplasmic reticulum (sER) are also shown in the cytoplasm. Lipid droplets (Li) appear smaller than those seen in Group IV. One cytoplasmic vacuole (V) is still noticed in the cytoplasm (TEM, ×2000)

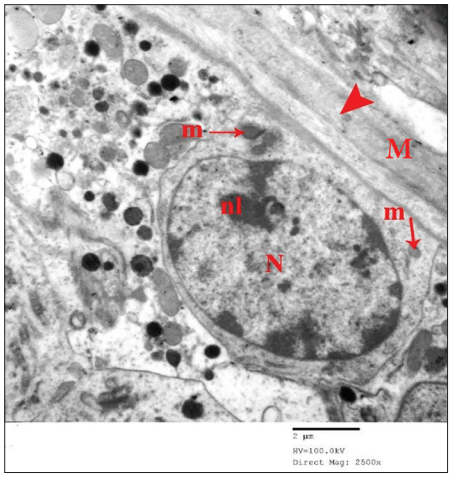

Figure 30: Electron photomicrograph of a spermatogonium from Group V, nearly similar to the control group. It rests on a regular thin basement membrane (arrowhead) that shows a flat myoid cell (M) with its flat nucleus. It has a regular oval nucleus (N) with few condensed chromatin arranged peripherally and around the nucleolus (nl). Some mitochondria (m) are shown in the cytoplasm (TEM, ×2500)

animals (90%) when compared to group IV. The tubules were separated by narrow interstitial spaces, similar to that of the control group. Most of the Leydig cells were normal except for few cells that were shrunken and had pyknotic nuclei.

Most of the seminiferous tubules appeared regular with well-defined basement membrane, lined with all germinal cells and filled with sperms. However, few of the counted tubules appeared shrunken, had partial loss of the germinal epithelium, and showed corrugations in some areas of their basement membrane and/or areas of detachment of the germinal epithelium from the basement membrane. Very few seminiferous tubules showed extensive loss of germinal epithelium. The frequency distribution of all the histopathological changes in this group is shown in Table 1. Statistical analysis showed a significant increase in the mean thickness of the germinal epithelium and the mean diameter of the seminiferous tubules, compared to that of the Cis group [Figure 3 and Table 2].

Group VI (Cis + RJ) also showed evidence of improvement. Compared to the control group, most of the animals of Group VI (Cis + RJ) showed preserved architecture of the testis with thin tunica albuginea and narrow interstitial spaces similar to that of the control group. Few Leydig cells were necrotic. Most of the seminiferous tubules of this group were regular with well-defined basement membrane, lined with all layers of germinal epithelium and filled with sperms. Few tubules were shrunken, had partial loss of the germinal epithelium, and had corrugations in some areas of the basement membrane and areas of detachment of the germinal epithelium from its basement membrane. Very few tubules showed extensive loss of germinal epithelium. There was a significant increase in the mean thickness of the germinal epithelium and the mean diameter of the seminiferous tubules, compared to that of the Cis group. The frequency distribution of all changes in this group is shown in Tables 1 and 2.

All the statistical data in this group were significantly less than that of the Cis Group (IV). Although the percentages of the different histopathological changes in this group (Cis + RJ) were more than that of Group V (Cis + Nanoselenium), there was no statistically significant difference between both groups [Figure 4 and Table 3].

Masson's trichrome results

Groups I, II, and III showed the normal greenish color of the connective tissue of the tunica albuginea and the walls of the seminiferous tubules [Figure 5]. While Group IV (Cis) showed greenish thickened tunica albuginea with irregular fibers and thickened walls of the blood vessels [Figure 6], Group V (Cis + Nanoselenium) and Group VI (Cis + RJ) showed nearly similar results to that of the control group [Figures 7 and 8].

Periodic acid–Schiff results

Groups I, II, and III showed PAS + ve regular basement membrane, in addition to PAS + ve caps of early spermatid and heads of late spermatids [Figure 9]. Group IV (Cis) showed corrugated PAS + ve basement membrane with areas of separation from the germinal epithelium and thickening [Figure 10]. Groups V and VI showed PAS + ve, almost, regular basement membrane with few areas of corrugations in addition to PAS + ve caps of early spermatids and heads of late spermatids [Figures 11 and 12].

Caspase-3 immunostaining results

Groups I, II, and III showed almost negative immunoreactivity in the cytoplasm of the germinal epithelium cells and Leydig cells with a color area percentage of 1.8% of the brown-colored immunoreaction [Figures 13 and Graph 2]. Group IV showed strong brown cytoplasmic immunoreactivity of the germinal epithelium cells and Leydig cells with a mean color area percentage of 56.5% and a mean optical density of 0.7 [Figure 14 and Graphs 2, 3]. Groups V and VI showed significant weak cytoplasmic immunoreactivity of the germinal epithelium cells and Leydig cells, compared to Group IV. The mean color area percentage of the brown immunoreaction was 27% in Group V and 31.5% in Group VI, and the mean optical density was 0.29 in Group V and 0.34 in Group IV [Figures 15, 16 and Graphs 2 and 3]. There was no significant difference between Group V and Group VI [Table 3].

Transmission electron microscopic results

The control group showed normal appearance of the seminiferous tubules and germinal epithelium [Figures 17-21]. In addition, Leydig cells showed normal picture [Figure 22].

Groups II and III showed testicular sections similar to those of the control group.

Table 3: Difference in the weight of the testes, mean optical density, and color area percentage of caspase-3 immunoreactivity and all assessed parameters of the seminiferous tubules (median and range) between Groups V and VI

	Median (range)		*P*
	Group V	Group VI	
Weight of testes	1.2 (1-1.5)	1.1 (0.88-1.45)	1
Mean optical density	0.29 (0.28-0.31)	0.32 (0.3-0.45)	1
Color area percentage	24.7 (20.3-29.5)	27.5 (23.6-33.7)	1
Assessment of qualitative parameters (%) of the seminiferous tubules			
Basement membrane corrugation	23.3 (13.3-30)	28.3 (16.7-40)	1
Separation of germinal epithelium from the basement membrane	21.7 (13.3-30)	28.3 (10-43.3)	1
Separation of germinal epithelium cells from each other	20 (13.3-30)	26.7 (20-36.7)	1
Partial loss of germinal epithelium	21.66 (6.7-33.3)	26.7 (13.3-40)	1
Extensive loss of germinal epithelium	0 (0-13.3)	0 (0-16.7)	1
Sloughing of germinal epithelium cells into the lumen	11.66 (0-23.3)	13.3 (10-26.7)	1
Cytoplasmic vacuolation	30 (23-33.3)	30 (20-43.3)	1
Nuclear changes	30 (20-33.3)	30 (16.7-43.3)	1
Shrinkage of seminiferous tubules	13.3 (10-23.2)	13.4 (6.7-33.3)	1
Assessment of quantitative parameters of the seminiferous tubules			
Diameter of seminiferous tubules	238.7 (209.6-246.2)	237.4 (228.9-261.9)	1
Thickness of germinal epithelium	57.4 (40.6-72.9)	60 (44.9-66.1)	1

Group IV (Cis) showed necrosis of the germinal epithelium and Leydig cells in the form of cytoplasmic vacuolations, pyknosis, fragmented chromatin, or loss of nuclei. Sertoli cells showed shrunken eccentric nuclei and vacuolated cytoplasm that contained large electron-dense lipid droplets [Figure 23]. The spermatogonia showed dark shrunken irregular nuclei and vacuolations of the cytoplasm. The cells were detached from the basement membrane and were separated from the neighboring cells [Figure 24]. Primary spermatocytes showed irregular nuclei with dark fragmented chromatin. The cytoplasm showed disintegration and vacuolation [Figure 25]. Early spermatids showed shrunken, rounded-to-oval nuclei that lacked acrosomal caps. Their cytoplasm was massively vacuolated, and the remnants of cytoplasm contained few mitochondria [Figure 26]. Late spermatids were deformed with decreased condensation of their nuclei. Their caudal parts lacked the elongating tails [Figure 27]. Leydig cells showed irregular, dark, shrunken nuclei and vacuolated cytoplasm that had multiple lysosomes and few mitochondria, but no lipid droplets were shown [Figure 28].

Group V (Cis + Nanoselenium) showed evidence of improvement of the testicular sections. The cell population was apparently increased with preservation of the architecture, compared to that of Group IV. The cells were in close contact with each other except for few areas of separation. Most of the germinal epithelium cells were nearly similar to those of the control group [Figures 29-33]. However, few vacuoles were still noticed in the cytoplasm of Sertoli cells in addition to electron-dense lipid droplets which were smaller than those seen in Cis group but larger than those of the control group [Figure 29]. Early spermatids appeared nearly normal in shape, but some cells showed few areas of separation from the neighboring cells [Figure 32]. Leydig cells showed nuclei and organelles, nearly similar to those of the control group. However, no lipid droplets were shown in their cytoplasm [Figure 34].

Group VI showed also evidence of improvement. The findings of this group were nearly similar to those detected in Group V. Most of the germinal epithelium cells showed evidence of improvement [Figures 35-39]. However, few vacuoles were still noticed in the cytoplasm of Sertoli cells, which also showed electron-dense lipid droplets, smaller than those seen in Group IV but larger than those of Group I [Figure 35]. Few vacuoles were noticed in the cytoplasm of primary spermatocytes [Figure 37] and most of the cells showed few areas of separation from the neighboring cells. Leydig cells showed nuclei and organelles nearly similar to those of the control group. However, no lipid droplets were seen [Figure 40].

Discussion

In this study, selenium nanoparticles were used instead of selenium because of its reported lower toxicity and higher antioxidant effects.[7] We also used RJ due to its proved antioxidant effects in animal model of oxidative stress condition induced by different substances such as bleomycin, methotrexate, and Cis.[12]

In the present study, the weight of testes of the Cis group significantly decreased compared to that of the control group. Similar results were described by other researchers[13] who used a similar Cis dose as ours. The decreased weight was attributed to marked parenchymal atrophy, loss of maturation of the germinal cells and necrosis, reduced germinal cell thickness, and tubular shrinkage of testicular tissues.[14,15]

H and E-stained testicular sections of the Cis group showed loss of testes architecture, widening of the interstitial spaces

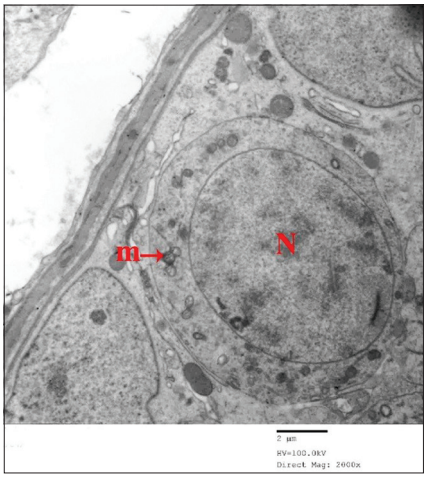

Figure 31: Electron photomicrograph of a primary spermatocyte from Group V, nearly similar to the control group. The cell is large with a central large regular rounded nucleus (N) in the prophase stage of the first meiotic division. The cytoplasm shows numerous mitochondria (m) (TEM, ×2000)

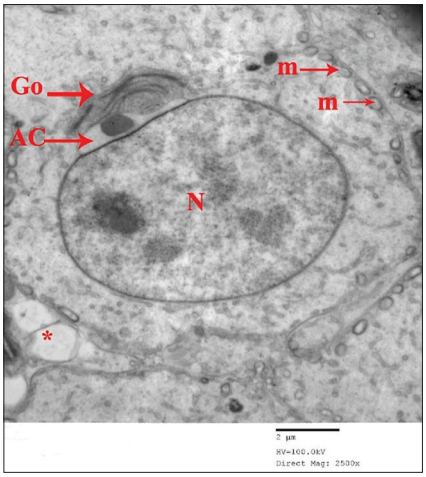

Figure 32: Electron photomicrograph of an early spermatid from Group V, nearly similar to that of the control group. It shows a rounded cell with rounded-to-oval nucleus (N) covered anteriorly with an acrosomal cap (AC). The nucleus occupies most of the cytoplasm that shows numerous mitochondria (m) arranged peripherally, and a Golgi apparatus (Go) is shown near the nucleus. Areas of separation between cells are still present (asterisk) (TEM, ×2500)

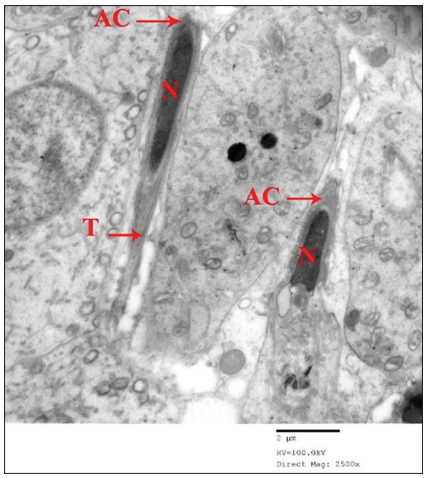

Figure 33: Electron photomicrograph of two late spermatids from Group V, nearly similar to that of the control group. The spermatid is formed from almost a pyriform electron-dense nucleus (N) covered anteriorly with an acrosomal cap (AC). The caudal parts of spermatids show the elongating tail (T) (TEM, ×2500)

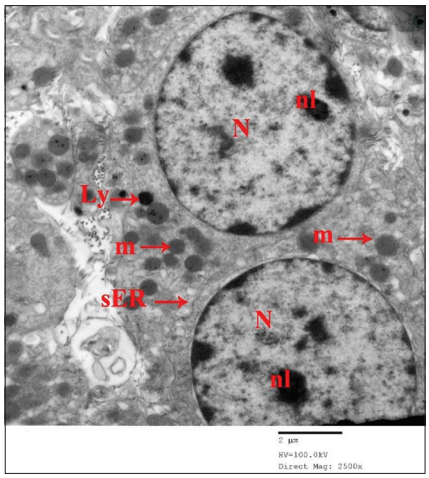

Figure 34: Electron photomicrograph of two Leydig cells from Group V showing evidence of improvement. Each one has a regular rounded nucleus (N), with predominant euchromatin and a nucleolus (nl). The cytoplasm shows numerous mitochondria (m) and well-developed smooth endoplasmic reticulum (sER). No lipid droplets are shown (TEM, ×2500)

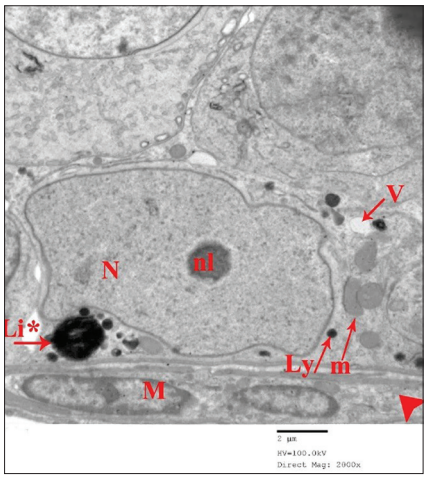

Figure 35: Electron photomicrograph of a Sertoli cell from Group VI showing evidence of improvement. It rests on a regular basement membrane (arrowhead) that shows flat myoid cells (M) with flat nuclei. It shows a large indented euchromatic nucleus (N) with a prominent nucleolus (nl). The cytoplasm shows mitochondria (m) and lysosomes (Ly). One cytoplasmic vacuole and a large electron-dense lipid droplet (Li) are still noticed in the cytoplasm. Minimal separation of the cell (asterisk) from the neighboring cell is present (TEM, ×2000)

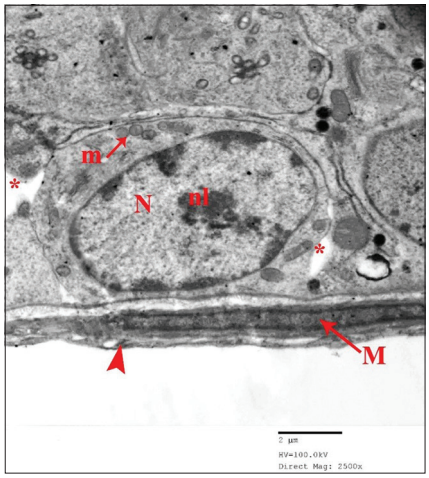

Figure 36: Electron photomicrograph of a spermatogonium from the Group VI showing evidence of improvement. It rests on a regular basement membrane (arrowhead) that shows a flat myoid cell (M) with a flat nucleus. It has a regular oval nucleus (N) with condensed chromatin arranged peripherally and around the nucleolus (nl). Some mitochondria (m) are shown in the cytoplasm. Few areas of separation (asterisk) from the surrounding cells are shown (TEM, ×2500)

between the seminiferous tubules, and congestion of the blood vessels. These results are consistent with previous studies.[16]

The congestion of blood vessels was reported to be a sign of inflammation associated with the administration of Cis, due to increased level of nuclear factor kappa-light-chain-enhancer of activated B cells. In addition, the wide interstitial spaces reflect the interstitial edema caused by the effect of Cis on endothelial cells, causing telangiectasia followed by endothelial disruption and fluid transudation. Moreover, it was reported that excessive production of nitric oxide by Cis causes vasodilatation and hypotension, leading to organ hypoperfusion and edema. In addition, decrease in testosterone production after Cis treatment could directly or indirectly affect the interstitial tissue and lymphatic space, provoking interstitial testicular edema.[5,14,16]

The seminiferous tubules of this group were shrunken, were irregular, had corrugated basement membrane, and had partial or extensive loss of the germinal epithelium. Leydig cell nuclei were pyknotic. These results are consistent with previous results[13,17] that used the same dose of Cis as ours. Our TEM examination confirmed the H and E results and those reported in other studies.[4,16]

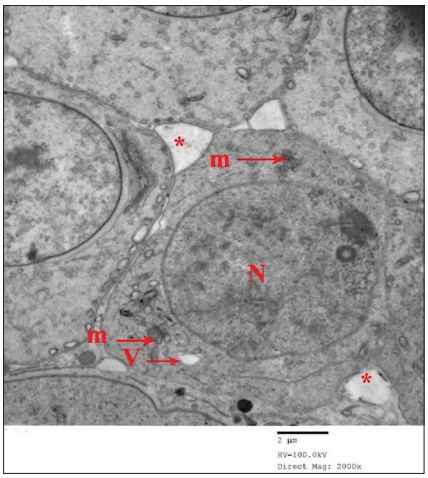

Figure 37: Electron photomicrograph of a primary spermatocyte from the Group VI showing evidence of improvement. The cell is large with a central, large, regular, rounded nucleus (N) in the prophase of the first meiotic division. The cytoplasm shows numerous mitochondria (m). One cytoplasmic vacuole (V) and few areas of separation (*) from the neighboring cells are shown (TEM, ×2000)

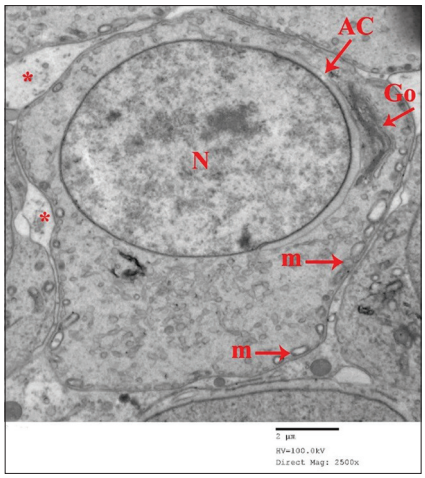

Figure 38: Electron photomicrograph of an early spermatid from the Group VI showing evidence of improvement. It shows a rounded cell with rounded-to-oval nucleus (N) covered anteriorly with an acrosomal cap (AC). The nucleus occupies most of the cytoplasm that shows numerous mitochondria (m) arranged peripherally, and a Golgi apparatus (Go) is shown near the nucleus. Areas of separation from the neighboring cells are shown (*) (TEM, ×2500)

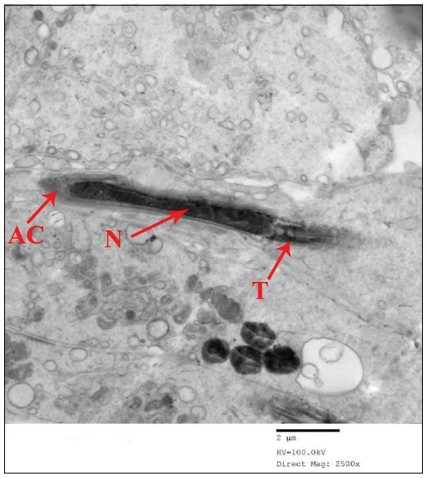

Figure 39: Electron photomicrograph of a late spermatid from the Group VI, nearly similar to that of the control group. It shows an elongated electron-dense nucleus (N) covered anteriorly with an acrosomal cap (AC). The caudal part of the spermatid shows the elongating tail (T) (TEM, ×2500)

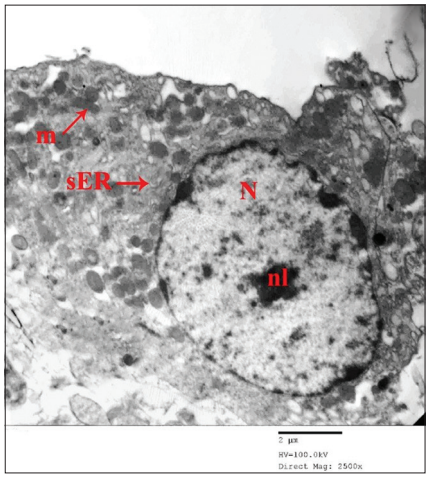

Figure 40: Electron photomicrograph of a Leydig cell from the Group VI, nearly similar to that of the control group. It shows a regular, almost rounded nucleus (N), with a predominant euchromatin and a nucleolus (nl). The cytoplasm shows smooth endoplasmic reticulum (sER) and numerous mitochondria (m). No lipid droplets are shown (TEM, ×2500)

The detected corrugation of the basement membrane appeared in our study, could be the result of myoid cell contraction or the reduction of tubular diameter.[18] This contraction might be the result of increased endothelin-1 protein produced by endothelial cells and vascular smooth muscle cells.[19] It was found that Cis caused a significant increase in this protein production in the testicular tissues of adult male Wistar rats.[20]

The detected germinal epithelium loss could be the result of apoptosis, necrosis, and the arrest of spermatogenic cells at various stages of division.[21] The germinal epithelium vacuolated cytoplasm could be attributed to lipid peroxidation caused by Cis. Moreover, the detachment of the germinal epithelium cells from the basement membrane and from each other could be attributed to different mechanisms such as loss of cadherin, damage of the blood–testis barrier tight junctions caused by lipid peroxidation,[16,18] and the reduction in testosterone hormone required for the attachment of different generations of germ cells within the seminiferous tubules.[22]

Sertoli cells showed large electron-dense lipid droplets in their cytoplasm. Similar finding was described in a previous study on using gibberellic acid which also causes oxidative stress and apoptosis.[23] It was documented that Sertoli cells phagocytose, degrade apoptotic cells, and store residual lipids within lipid

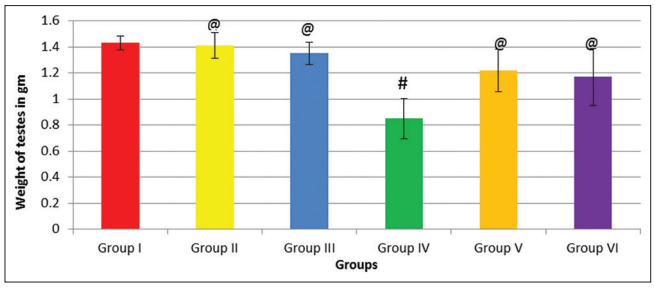

Graph 1: Weight of the testes among the six experimental groups presented as mean ± standard deviation. Kruskal–Wallis test, *post hoc* pairwise comparisons used adjusted Bonferroni approach. Statistically significant at $P < 0.05$. #Statistically significant when compared with Group I; @Statistically significant when compared with Group IV

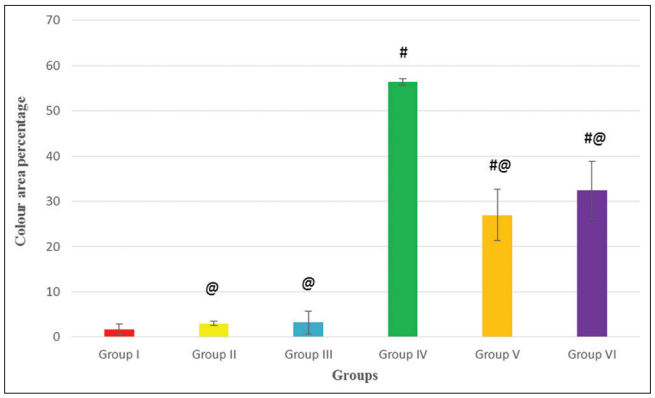

Graph 2: Color area percentage of caspase-3 immunoreactivity among the six experimental groups presented as mean ± standard deviation. Kruskal–Wallis test, *post hoc* pairwise comparisons used adjusted Bonferroni approach. Statistically significant at $P < 0.05$. #Statistically significant compared to Group I; @Statistically significant compared to Group IV

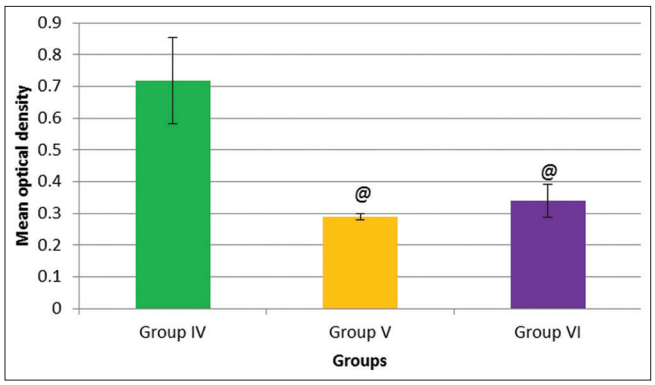

Graph 3: Mean optical density of caspase-3 immunoreactivity among IV, V, and VI groups presented as mean ± standard deviation. Kruskal–Wallis test, *post hoc* pairwise comparisons used adjusted Bonferroni approach. Statistically significant at $P < 0.05$. @Statistically significant when compared with Group IV

droplets. Thus, the observed increase in lipid droplets in our study could indicate increased apoptosis.[23]

Early spermatids showed lack of acrosomal caps, whereas late spermatids were deformed with decreased condensation of their nuclei and lost elongating tails. These findings were consistent with a study that found head deformity and tail abnormalities including absent tails in sperms following daily treatment with Cis for 60 days.[24] These deformations were reported to be due to Cis-induced DNA damage in germ cells, leading to altered sperm morphology.[25]

The apparent decrease in mitochondria in Leydig cells and some germinal cells, found in our study, could be attributed to direct mitochondrial damage by Cis as it forms adducts with mitochondrial DNA, leading to inhibition of mitochondrial DNA replication.[13] No lipid droplets were found in the cytoplasm of Leydig cells, which could be due to: first, Cis decreased of the expression of the transmembrane protein (SRB1) which is involved in cholesterol uptake, leading to decrease in the intracellular transport of cholesterol, the substrate of testosterone synthesis, which is stored in the lipid droplets[26,27] and second, *de novo* synthesis of cholesterol inside the cell begins from the acetyl-CoA, which is transported from the mitochondria to the cytosol.[28] Thus, the absence of lipids can be a consequence of the decreased cholesterol synthesis due to mitochondrial damage caused by Cis.

The increased deposition of collagen in tunica albuginea and the walls of the blood vessels showed in Masson's trichrome-stained sections of the Cis group is also shown in other studies.[16] This increase could be explained by the activation of p38 mitogen-activated protein kinase by reactive oxygen species, which in turn induces fibrosis caused by the transforming growth factor-β1 (TGF-β1).[14]

PAS-stained sections of the Cis group revealed thickening of the basement membrane, which was confirmed by TEM results. Similar findings were described by other researchers[18] who attributed the thickening to either increased production of the basement membrane by Sertoli and myoid cells or decreased proteolysis rate in the extracellular matrix.

In this group, there was strong caspase-3 immunoreactivity in the germinal epithelium and Leydig cells, which was confirmed by increased color area percentage of this immunoreactivity, compared to that of the control group. This may reflect increased apoptosis induced by Cis. Similar results were found by other researchers.[21] Cis activates caspase3 via the extracellular signal-regulated kinase pathway. The caspase cascade induces apoptosis, leading to DNA fragmentation, chromatin condensation, and destruction of bio-membrane protein.[3,29]

Overall, Cis-induced histopathological alterations detected by LM and TEM examinations can be explained by the imbalance between oxidants and antioxidants in the testicular tissue. Cis increased the level of ROS and free radicals which damaged cellular lipids, proteins and DNA and promoted necrosis. In addition, Cis-induced excessive production of NO interacts with ROS to form peroxynitrite, which is a powerful oxidant and cytotoxic agent, resulting in more cellular damage.[4,9,29]

Moreover, Cis decreased the testicular activities of antioxidants

such as glutathione and catalase, which normally prevented the generation of ROS.[14] In addition, DNA formed intrastrand crosslinks and adducts, which inhibited DNA replication and/or transcription and activated several signal transduction pathways, leading to activation of apoptosis.[14,30]

In the group of Cis + Nano Se, there was a significant restoration of the testes weight, compared to that of the Cis group. This was also noticed in a previous study that used Nano Se in the same dose and duration. The researchers attributed this weight restoration to the androgenic effect of Nano Se on the testis.[9]

H and E-stained testicular sections of this group showed preserved architecture of the testes with a significant decrease in all histopathologic parameters compared to that of the Cis group. However, most of the improved parameters did not return significantly to the control levels, denoting partial protection. These results are consistent with those of other researchers[9] who used Nano Se in the same dose and duration against Cis-induced testicular damage.

The protection caused by Nano Se may be related to its strong antioxidant properties as Se is a central component of glutathione peroxidase which degrades hydroperoxides and hydrogen peroxide. Besides, Nano Se is reported to protect against oxidative stress by blocking caspase-mediated apoptosis induced by Cis through inhibition of ROS overproduction[9] and increasing the free radical scavenger metallothionine-1 in testes.[8,31]

Aside from its antioxidant activity, Se increases the activity of both DNA repair enzymes and repair pathways.[32] The Nano Se has a positive effect on testosterone biosynthesis. It increases steroidogenic acute regulatory protein (StAR) levels, cholesterol side chain cleavage enzyme (P450scc/CYP11A1), and 17 β-hydroxysteroid dehydrogenase (17 β-HSD). STAR mediates cholesterol transport through the mitochondrial membrane. CYP11A1 converts mitochondrial cholesterol into pregnenolone and finally 17 β-HSD converts androstenedione to testosterone.[32] Meanwhile, Cis was reported to reduce those three enzymes.[33]

The H and E results of this group were confirmed by the TEM examination that showed improvement on the ultrastructure level, noticed by other researchers who used Nano Se against testicular toxicity caused by bisphenol.[34]

Sertoli cells showed smaller electron-dense lipid droplets than those seen in the Cis group but still larger than those of the control group. This could reflect the decreased apoptotic cells phagocytosed by Sertoli cells.[23]

Leydig cells were nearly similar to those of the control group. However, no lipid droplets were shown in their cytoplasm, reflecting lack of cholesterol stores in the cytoplasm. This could be due to restoration of testosterone synthesis by Nano Se,[32] leading to the detected loss of lipid droplets.[27]

The seminiferous tubule diameter and germinal epithelium thickness increased significantly compared to those of the Cis group, but still significantly less than those of the control group. This reflects the restored spermatogenesis. This was noticed by other researchers on using Se against monosodium glutamate-induced damage in rat testis.[35]

Masson's trichrome-stained sections of this group were nearly similar to those of the control group as detected in previous studies.[36,37] This could be the result of Nano Se's ability to scavenge free radicals and ROS produced by Cis, leading to suppression of the stimulatory effect of Cis on the fibrosing gene TGF-β1, as mentioned earlier. A previous study also reported that Se supplementation protected thyroid gland from TGF-β1-induced fibrosis.[38]

PAS-stained sections showed almost regular basement membrane with few areas of thickening. These findings were confirmed with TEM examination and are consistent with a study that used Nano Se intraperitoneally for 6 days against oxidative testicular damage caused by gentamycin in albino rats.[39]

The caspase-3 immunostained sections of this group showed weak caspase-3 immunoreactivity confirmed by decreased color area percentage as compared to that of the Cis group. These results are in concordance with other studies.[40] This could be due to the blockage of the caspase-mediated apoptosis by Nano Se.

The Cis + RJ group showed restoration of the testes weight compared to that of the Cis group. These findings are consistent with the findings of other researchers who reported that RJ alleviated the decreased testes weight caused by oxidative stress of cadmium toxicity.[41]

H and E-stained testicular sections of this group showed evidence of improvement, nearly similar to that of the Cis + Nano Se group, with significant decrease in all histopathologic parameters compared to those of the Cis group. However, most of the improved parameters did not return significantly to the control levels, denoting partial protection. This ameliorative effect was described by previous studies on using a similar RJ dose but with different toxic substances.[5,42]

RJ contains among its numerous beneficial constituents, free amino acids such as proline, cystine, and cysteine. Proline acts as an antioxidant due to its hydroxyl radical-scavenging activity. Meanwhile, cystine and cysteine participate in the synthesis of glutathione, which is an effective cellular antioxidant.[12] Another reported explanation RJ is that it increased the activity of antioxidant enzymes in tissues.[29] In addition, it contains spermatogenesis-stimulating substances such as Vitamin C, Vitamin E, and arginine.[43]

The H and E results of this group were confirmed by the TEM examination. The cells were in close contact with each other, and most of them were nearly similar to those of the control group. The ultrastructure of Sertoli cells and Leydig cells was nearly similar to that of the Cis + Nano Se group. The seminiferous tubule diameter and germinal epithelium thickness increased significantly compared to those of the Cis group, but they were still significantly less than those

of the control group, reflecting spermatogenesis restoration. These results were noticed by other researchers[5] with the administration of RJ in similar dose and duration against Cis toxicity.

Masson's trichrome-stained sections of this group were nearly similar to those of the control group. This decrease in collagen deposition by RJ against Cis was also noticed in the renal tissue of albino rats. Blocking TGF-β-1 expression by RJ resulted in the suppression of collagen production and subsequent modulation of fibrotic processes.[14]

PAS-stained sections showed almost regular basement membrane with few areas of thickening, similar to previous studies[44] which used RJ in different doses and found alleviation of testicular toxicity caused by aluminum chloride-induced oxidative stress, in a dose-dependent manner.

The detected weak caspase-3 immunoreactivity and decreased color area percentage caused by RJ were in harmony with a previous study[29] which found that RJ supplementation arrested the apoptotic progression and protected the testicular tissue against cadmium-induced testicular toxicity.

In this study, we did not find any statistically significant difference between the Nano Se + Cis and RJ + Cis groups. Although both of them are antioxidants, they have different mechanisms of action; both of them could increase testosterone synthesis and both of them could decrease the apoptosis induced by Cis. Thus, further studies are needed to explore their effects in different doses and durations.

Conclusion

Administration of both selenium nanoparticles at a dose of 2 mg/kg BW and RJ at a dose of 100 mg/kg BW daily for 10 days promoted partial improvement in the morphology and ultrastructure of testis against Cis-induced testicular toxicity in adult male albino rats with no statistically significant difference between them.

Financial support and sponsorship

Nil.

Conflicts of interest

There are no conflicts of interest.

References

1. Eid A. Protective effect of l-carnitine against cisplatin-induced testicular toxicity in rats. Al Azhar J Pharm Sci 2016;53:123-42.
2. Soni KK, Kim HK, Choi BR, Karna KK, You JH, Cha JS, *et al.* Dose-dependent effects of cisplatin on the severity of testicular injury in Sprague Dawley rats: Reactive oxygen species and endoplasmic reticulum stress. Drug Des Devel Ther 2016;10:3959-68.
3. Mercantepe T, Unal D, Tümkaya L, Yazici ZA. Protective effects of amifostine, curcumin and caffeic acid phenethyl ester against cisplatin-induced testis tissue damage in rats. Exp Ther Med 2018;15:3404-12.
4. Abdel-Mohsen A, Elgendy M, Elmarakby D, Eldsouky D. Histological study on the role of ginger against cisplatin induced testicular toxicity *in albino* rats. Egypt J Histol 2013;36:312-20.
5. Raafat M, Hamam G. The possible protective role of royal jelly against cisplatininduced testicular lesions in adult albino rats: A histological and immunohistochemical study. Egypt J Histol 2012;35:353-65.
6. Salem EA, Salem NA, Maarouf AM, Serefoglu EC, Hellstrom WJ. Selenium and lycopene attenuate cisplatin-induced testicular toxicity associated with oxidative stress in Wistar rats. Urology 2012;79:1184.e1-6.
7. Asri-Rezaei S, Nourian A, Shalizar-Jalali A, Najafi G, Nazarizadeh A, Koohestani M, *et al.* Selenium supplementation in the form of selenium nanoparticles and selenite sodium improves mature male mice reproductive performances. Iran J Basic Med Sci 2018;21:577-85.
8. Abd-Allah S, Hashem KS. Selenium nanoparticles increase the testicular antioxidant activity and spermatogenesis in male rats as compared to ordinary selenium. Int J Adv Res 2015;3:792-802.
9. Rezvanfar MA, Rezvanfar MA, Shahverdi AR, Ahmadi A, Baeeri M, Mohammadirad A, *et al.* Protection of cisplatin-induced spermatotoxicity, DNA damage and chromatin abnormality by selenium nano-particles. Toxicol Appl Pharmacol 2013;266:356-65.
10. Najafi G, Nejati V, Shalizar Jalali A, Zahmatkesh E. Protective role of royal jelly in oxymetholone-induced oxidative injury in mouse testis. Iran J Toxicol 2014;8:1073-80.
11. Queiroz G, Oliveira VV, de Gueiros OG, Torres SM, de Maia FC, Tenorio BM, *et al*. Effect of pentoxifylline on the regeneration of rat testicular germ cells after heat shock. Anim Reprod 2013;10:45-54.
12. Kocot J, Kiełczykowska M, Luchowska-Kocot D, Kurzepa J, Musik I. Antioxidant potential of propolis, bee pollen, and royal jelly: Possible medical application. Oxid Med Cell Longev 2018;2018:7074209.
13. Fekry E, Rahman AA, Awny MM, Makary S. Protective effect of mirtazapine versus ginger against cisplatin-induced testicular damage in adult male albino rats. Ultrastruct Pathol 2019;43:66-79.
14. Ibrahim NA. The possible protective effect of bee propolis on experimentally mediated cisplatin reproductive toxicity: A histological and immunohistochemical study. Egypt J Histol 2013;36:78-86.
15. Akunna G, Obikili E, Anyawu GE, Esom E. Histochemical and morphometric evidences of the curative role of aqueous zest extract of *Citrus sinensis* on anti-neoplastic drug-induced testicular degeneration in animal models. Eur J Anat 2018;22:497-507.
16. Meligy FY, Abo Elgheed AT, Alghareeb SM. Therapeutic effect of adipose-derived mesenchymal stem cells on Cisplatin induced testicular damage in adult male albino rat. Ultrastruct Pathol 2019;43:28-55.
17. Jahan S, Munawar A, Razak S, Anam S, Ain QU, Ullah H, *et al.* Ameliorative effects of rutin against cisplatin-induced reproductive toxicity in male rats. BMC Urol 2018;18:107.
18. Mohammadnejad D, Abedelahi A, Soleimani-Rad J, Mohammadi-Roshandeh A, Rashtbar M, Azami A. Degenerative effect of cisplatin on testicular germinal epithelium. Adv Pharm Bull 2012;2:173-7.
19. Kowalczyk A, Kleniewska P, Kolodziejczyk M, Skibska B, Goraca A. The role of endothelin-1 and endothelin receptor antagonists in inflammatory response and sepsis. Arch Immunol Ther Exp (Warsz) 2015;63:41-52.
20. Hamza AA, Elwy HM, Badawi AM. Fenugreek seed extract attenuates cisplatin-induced testicular damage in Wistar rats. Andrologia 2016;48:211-21.
21. Karimi S, Hosseinimehr SJ, Mohammadi HR, Khalatbary AR, Amiri FT. *Zataria multiflora* ameliorates cisplatin-induced testicular damage via suppression of oxidative stress and apoptosis in a mice model. Iran J Basic Med Sci 2018;21:607-14.
22. Khafaga AF, Bayad AE. Impact of *Ginkgo biloba* extract on reproductive toxicity induced by single or repeated injection of cisplatin in adult male rats. Int J Pharmacol 2016;12:340-50.
23. Regueira M, Gorga A, Rindone GM, Pellizzari EH, Cigorraga SB, Galardo MN, *et al.* Apoptotic germ cells regulate Sertoli cell lipid storage and fatty acid oxidation. Reproduction 2018;156:515-25.
24. Elballat SE. Protective effect of curcumin and Vitamin C each alone and in combination on cisplatin-induced sperm abnormalities in male albino rats. J Basic Appl Zool Cell Biol Genet 2016;76:52-9.
25. Bagheri-Sereshki N, Hales BF, Robaire B. The effects of chemotherapeutic agents, bleomycin, etoposide, and cisplatin, on chromatin remodeling in male rat germ cells. Biol Reprod 2016;94:81.

26. Kilarkaje N. Effects of combined treatment of α-tocopherol, L-ascorbic acid, selenium and zinc on bleomycin, etoposide and cisplatin-induced alterations in testosterone synthesis pathway in rats. Cancer Chemother Pharmacol 2014;74:1175-89.
27. Ojo OO, Omolola O, Tosin OB. Quercetin controlled cytarabine-induced testicular damage in Swiss albino mice 1. Int J Adv Res Biol Sci 2019;6:1-13.
28. Sèdes L, Thirouard L, Maqdasy S, Garcia M, Caira F, Lobaccaro JA, *et al.* Cholesterol: A gatekeeper of male fertility? Front Endocrinol (Lausanne) 2018;9:369.
29. Almeer RS, Abdel Moneim AE. Evaluation of the protective effect of olive leaf extract on cisplatin-induced testicular damage in rats. Oxid Med Cell Longev 2018;2018:8487248.
30. Petrović M, Todorović D. Biochemical and molecular mechanisms of action of cisplatin in cancer cells. Facta Universitatis, Series: Medicine & Biology 2016;18:12-8.
31. Yildiz A, Kaya Y, Tanriverdi O. Effect of the interaction between selenium and zinc on DNA repair in association with cancer prevention. J Cancer Prev 2019;24:146-54.
32. Gan X, Zhang X, Qiannan E, Zhang Q, Ye Y, Cai Y, *et al.* Nano-selenium attenuates nickel-induced testosterone synthesis disturbance through inhibition of MAPK pathways in Sprague-Dawley rats. Environ Toxicol 2019;34:968-78.
33. Tian M, Liu F, Liu H, Zhang Q, Li L, Hou X, *et al.* Grape seed procyanidins extract attenuates Cisplatin-induced oxidative stress and testosterone synthase inhibition in rat testes. Syst Biol Reprod Med 2018;64:246-59.
34. Halim BR, Khalaf AA, Moselhy WA, Ahmed WM. Protective effect of nano-selenium and ionized selenium against the testicular damage, endocrine disruptor and testicular ultrastructure of bisphenol A *in albino* male rats. Asian J Anim Vet Adv 2016;11:653-64.
35. Adegoke EO, Wang X, Wang H, Wang C, Zhang H, Zhang G. Selenium (Na_2SeO_3) upregulates expression of immune genes and blood-testis barrier constituent proteins of bovine Sertoli cell *in vitro*. Biol Trace Elem Res 2018;185:332-43.
36. Desouky MA, Mahmoud MA, Ahmed SM, Abo-Bakre AH. Histological and ultrastructural study of the protective effect of antioxidants on the testis of adult albino rat after treatment with aluminium chloride. Malays J Med Res 2014;25:89-113.
37. Sarhan NR. The Ameliorating effect of sodium selenite on the histological changes and expression of caspase-3 in the testis of monosodium glutamate-treated rats: Light and electron microscopic study. J Microsc Ultrastruct 2018;6:105-15.
38. Hanadi BA, Hakeem A, Kelany ME, Ameen HA, Karium SA. The possible protective role of antioxidants (selenium, Vitamin E) in reducing smoking effects on testes of albino rats. Assiut Univ B u l l Environ Res 2011;14:61-76.
39. Stuss M, Michalska-Kasiczak M, Sewerynek E. The role of selenium in thyroid gland pathophysiology. Endokrynol Pol 2017;68:440-65.
40. Hamoud A. Possible role of selenium nano-particles on gentamicin-induced toxicity in rat testis: Morphological and morphometric study. Egypt J Histol 2019;42:861-73.
41. Simsek N, Koc A, Karadeniz A, Yildirim ME, Celik HT, Sari E, *et al.* Ameliorative effect of selenium in cisplatin-induced testicular damage in rats. Acta Histochem 2016;118:263-70.
42. Ahmed MM, El-Shazly SA, Alkafafy ME, Mohamed AA, Mousa AA. Protective potential of royal jelly against cadmium-induced infertility in male rats. Andrologia 2018;50:e12996.
43. Silici S, Ekmekcioglu O, Eraslan G, Demirtas A. Antioxidative effect of royal jelly in cisplatin-induced testes damage. Urology 2009;74:545-51.
44. Mahdivand N, Nejati V, Najafi G, Shalizar Jalali A, Rahmani F. The protective effect of royal jelly on testicular histomorphometry and spermatogenesis in heat-stress exposed male rats. J Ilam Univ Med Sci 2019;26:69-78.